LITERATURE CITED

1. M. N. Gaidukov, N. V. Churaev, and Yu. I. Yalamov, "Toward a theory of liquid evaporation from capillaries at temperatures exceeding the boiling point", Zh. Tekh. Fiz., 46, No. 10, 2142-2146 (1976).
2. V. G. Levich, Physicochemical Hydrodynamics, Prentice-Hall (1962).
3. S. N. Zotov, Ya. I. Rabinovich, and N. V. Churaev, "Experimental study of high-temperature evaporation of liquids from capillaries", Inzh.-Fiz. Zh., 46, No. 6, 1035-1039 (1978).
4. R. Reed and T. Sherwood, Properties of Gases and Liquids [Russian translation], Khimiya, Leningrad (1971).
5. N. V. Pavlyukevich, G. E. Gorelik, V. V. Levdanskii, et al., Physical Kinetics and Transport Processes in Phase Conversions [in Russian], Nauka i Tekhnika, Minsk (1980).
6. N. I. Gamayunov, V. L. Malyshev, and A. S. Fel'dblyum, "The transitional regime of high-intensity liquid evaporation from a capillary", Inzh.-Fiz. Zh., 44, No. 2, 231-235 (1983).

NONSTEADY HEAT AND MOISTURE TRANSFER IN CAPILLARY-POROUS COLLOIDAL BODIES WITH CONVECTIVE DRYING

B. A. Todorov

UDC 66.047.37

A mathematical model describing the distribution of moisture content in the region of a moist state of capillary-porous colloidal bodies is proposed.

Formulation of the Problem

The drying of moist capillary-porous colloidal bodies is a typical nonsteady process occurring in the presence of transfer-potential gradients. The moisture-transfer potential for the given bodies is assumed to be the chemical potential of water vapor as a function of the temperature and partial pressure of the vapor. In the hygroscopic region, it may be expressed using the temperature and moisture content of the body. Taking this into account, the system of differential equations

$$\frac{\partial t}{\partial \tau} = a\nabla^2 t + \frac{\varepsilon r_0}{C}\frac{\partial U}{\partial \tau}, \tag{1}$$

$$\frac{\partial U}{\partial \tau} = D\nabla^2 U + D\delta\nabla^2 t, \tag{2}$$

describing the interrelated phenomena of heat and moisture transfer, was derived in [1]. Numerous solutions of this system of equations with different boundary conditions are found to be in good agreement with the experimental results of [2-7].

For wet bodies, the chemical potential is equal to the potential of free water, i.e., it is constant and cannot be used as the moisture-transfer potential. This explains the considerable deviation in the moisture-content distribution obtained from the solution of Eq. (2) from the experimental values in [2-7].

A mathematical model derived under the following assumptions is proposed to describe the moisture distribution in capillary porous bodies:

1) the transfer of capillary-bound water is not diffusional;

2) capillary-bound water is characterized by a density ρ, which is equal to the mass of this water per unit volume of the body;

3) nonsteady transfer of the moisture occurs under the influence of the combined action of the motive forces (pressure and temperature gradients, capillary potential, etc.). It is assumed that the resulting flux may be expressed using the rate of transfer $\vec{v}_{cap}$ and the density ρ by the equation

Higher Wood-Technology Institute, Sofia. Translated from Inzhenerno-Fizicheskii Zhurnal, Vol. 47, No. 4, pp. 651-657, October, 1984. Original article submitted June 9, 1983.

0022-0841/84/4704-1225$08.50

$$\vec{J}_{cap}=\rho\vec{v}_{cap}=\sum_{1}^{k}L_{ik}\vec{X}_k$$

or equivalently

$$\vec{J}_{cap}=\rho_0 U\vec{v}_{cap} \quad (3)$$

After substituting the expression for $\vec{J}_{cap}$ from Eq. (3) into the mass-conservation equation

$$\frac{\partial\rho}{\partial\tau}+\nabla\vec{J}=0 \quad (4)$$

and performing simple manipulations, a differential equation of hyperbolic type is obtained

$$\frac{\partial U}{\partial\tau}+\vec{v}_{cap}\nabla U=0,\quad \nabla\vec{v}_{cap}=0. \quad (5)$$

Since convective drying is widely used in practice, it is of interest to solve Eqs. (1) and (2) and (5) with boundary conditions of the third kind

$$\alpha(t_a-t_s)-\lambda(\nabla t)_s-(1-\varepsilon)r_0\alpha_u\rho_0(U_s-U_e)=0, \quad (6)$$

$$\alpha_u(U_s-U_e)+D(\nabla U)_s+D\delta(\nabla t)_s=0. \quad (7)$$

Numerical Solution of the Model

The solution of the problem is obtained by the finite-difference method in a rectangular two-dimensional grid with I × J points over the spatial coordinates. The two-step Laks–Vendorf scheme with second-order accuracy with respect to the time [3] is used to solve Eq. (5).

The auxiliary step in the Laks scheme for the given case takes the form

$$U_{ij+1}^{n+\frac{1}{2}}=\frac{1}{4}(U_{ij}^n+U_{i+1\,j+1}^n+U_{ij+2}^n+U_{i-1\,j+1}^n-\frac{\Delta\tau v_{cap}}{4\Delta}(U_{i+1\,j+1}^n-U_{i-1\,j+1}^n)-\frac{\Delta\tau v_{cap}}{4\Delta}(U_{ij+2}^n-U_{ij}^n), \quad (8)$$

$$U_{ij-1}^{n+\frac{1}{2}}=\frac{1}{4}(U_{ij-2}^n+U_{i+1\,j-1}^n+U_{ij}^n+U_{i-1\,j-1}^n)-\frac{\Delta\tau v_{cap}}{4\Delta}(U_{i+1\,j-1}^n-U_{i-1\,j-1}^n)-\frac{\Delta\tau v_{cap}}{4\Delta}(U_{ij}^n-U_{ij-2}^n), \quad (9)$$

$$U_{i+1j}^{n+\frac{1}{2}}=\frac{1}{4}(U_{i+1\,j-1}^n+U_{i+2j}^n+U_{i+1\,j+1}^n+U_{ij}^n)-\frac{\Delta\tau v_{cap}}{4\Delta}(U_{i+2j}^n-U_{ij}^n)-\frac{\Delta\tau v_{cap}}{4\Delta}(U_{i+1\,j+1}^n-U_{i+1\,j-1}^n), \quad (10)$$

$$U_{i-1j}^{n+\frac{1}{2}}=\frac{1}{4}(U_{i-1\,j-1}^n+U_{ij}^n+U_{i-1\,j+1}^n+U_{i-2j}^n)-\frac{\Delta\tau v_{cap}}{4\Delta}(U_{ij}^n-U_{i-2j}^n)-\frac{\Delta\tau v_{cap}}{4\Delta}(U_{i-1\,j+1}^n-U_{i-1\,j-1}^n). \quad (11)$$

The values of the vector components U defined in this way at fractional n + 1/2 moments of time are used in the difference equation, centered with respect to time and space; this leads to the basic step for calculating U at the n + 1 moment

$$U_{ij}^{n+1}=U_{ij}^n-\frac{\Delta\tau v_{cap}}{2\Delta}(U_{i+1j}^{n+\frac{1}{2}}-U_{i-1j}^{n+\frac{1}{2}})-\frac{\Delta\tau v_{cap}}{2\Delta}(U_{ij+1}^{n+\frac{1}{2}}-U_{ij-1}^{n+\frac{1}{2}}). \quad (12)$$

The system in Eqs. (1) and (2) is approximated by the Krank–Nikol'son implicit scheme, resulting in the implicit matrix equations

$$t_{ij}^{n+1}=t_{ij}^n+\frac{\mathrm{Fo}}{2}[(t_{i+1j}^{n+1}+t_{i-1j}^{n+1}+t_{ij+1}^{n+1}+t_{ij-1}^{n+1}-4t_{ij}^{n+1})+(t_{i+1j}^n+t_{i-1j}^n+t_{ij+1}^n+t_{ij-1}^n-4t_{ij}^n)]+\frac{r_0\varepsilon}{C}(U_{ij}^{n+1}-U_{ij}^n), \quad (13)$$

$$U_{ij}^{n+1}=U_{ij}^n+\frac{\mathrm{Fo}'}{2}[(U_{i+1j}^{n+1}+U_{i-1j}^{n+1}+U_{ij+1}^{n+1}+U_{ij-1}^{n+1}-4U_{ij}^{n+1})+(U_{i+1j}^n+U_{i-1j}^n+U_{ij+1}^n+U_{ij-1}^n-4U_{ij}^n)+$$
$$+\delta(t_{i+1j}^{n+1}+t_{i-1j}^{n+1}+t_{ij+1}^{n+1}+t_{ij-1}^{n+1}-4t_{ij}^{n+1})+\delta(t_{i+1j}^n+t_{i-1j}^n+t_{ij+1}^n+t_{ij-1}^n-4t_{ij}^n)], \quad (14)$$

where $\mathrm{Fo}=a\Delta\tau/\Delta^2$; $\mathrm{Fo}'=D\Delta r/\Delta^2$.

Matrix Eqs. (8)-(12) are stable if the Courant–Friedrichs–Levi condition is satisfied [3]

$$\Delta\tau\leqslant\Delta/(|v_{cap}|\sqrt{2}). \quad (15)$$

Analysis of the stability of the solution of matrix Eqs. (13) and (14) is undertaken using the vectorial Fourier mode

$$\hat{\mathbf{u}}=[\hat{t}^n\exp(ik_x x+ik_y y),\ \hat{U}^n\exp(ik_x x+ik_y y)]. \quad (16)$$

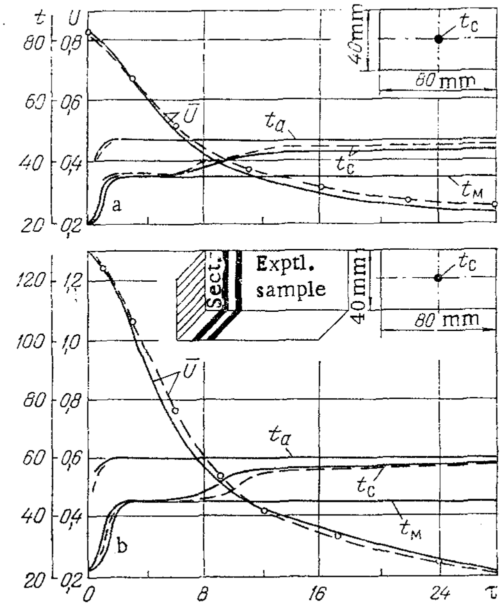

Fig. 1. Variation in moisture content $\bar{U}$ (kg/kg) and temperature t_c (°C) of experimental samples as a function of the time τ (h) with various experimental conditions: a) t_a = 47°C; t_M = 35°C; φ = 0.43; v_a = 5 m/sec; b) t_a = 60°C; t_M = 45°C; φ = 0.42; v_a = 5 m/sec; the continuous curves correspond to theory and the dashed curves to experiment.

Using the Fourier mode, a transition matrix G with two eigenvalues g_1, g_2 is obtained for Eqs. (13) and (14); g_1, g_2 may be less than unity. This means that the solution of the system of matrix equations must be stable for any values of Fo (Fo'). In fact, however, numerical experiment shows the presence of an oscillating solution when Fo (Fo') > 450.

The solution of matrix Eqs. (13) and (14) is obtained by the method of successive upper relaxation using Chebyshev polynomials to accelerate convergence in the early states of the iterative process [3]

$$t_{ij}^{(p+1)} = (1-\omega_t^{(p)})\, t_{ij}^{(p)} + \frac{\omega_t^{(p)}\mathrm{Fo}}{2(1+2\,\mathrm{Fo})}\left[(t_{i+1j}^{(p)} + t_{i-1j}^{(p+1)} + t_{ij+1}^{(p)} + t_{ij-1}^{(p+1)}) + \frac{2\varepsilon r_0}{C\,\mathrm{Fo}}\; U_{ij}^{(p)}\right] + \omega_t^{(p)} V_{ij}, \tag{17}$$

$$U_{ij}^{(p+1)} = (1-\omega_u^{(p)})\, U_{ij}^{(p)} + \frac{\omega_u^{(p)}\,\mathrm{Fo}'}{2(1+2\,\mathrm{Fo}')}\,[(U_{i+1j}^{(p)} + U_{i-1j}^{(p+1)} + U_{ij+1}^{(p)} + U_{ij-1}^{(p+1)} + \delta\,(t_{i+1j}^{(p)} + t_{i-1j}^{(p+1)} + t_{ij+1}^{(p)} + t_{ij-1}^{(p+1)} - 4t_{ij}^{(p)})] + \omega_u^{(p)} W_{ij}, \tag{18}$$

where

$$\omega^{(0)} = 1;\quad \omega^{(1)} = 1/(1-\mu_m^2/2);\quad \text{for}\quad p \geqslant 1\quad \omega^{(p+1)} = 1/(1-\mu_m^2\,\omega^{(p)}/4);$$

$$V_{ij} = \frac{1-2\,\mathrm{Fo}}{1+2\,\mathrm{Fo}}\, t_{ij}^{n} + \frac{\mathrm{Fo}}{2(1+2\,\mathrm{Fo})}\left(t_{i+1j}^{n} + t_{i-1j}^{n} + t_{ij+1}^{n} + t_{ij-1}^{n} - \frac{2\varepsilon r_0}{C\,\mathrm{Fo}} U_{ij}^{n}\right);$$

$$W_{ij} = \frac{1-2\,\mathrm{Fo}'}{1+2\,\mathrm{Fo}'}\, U_{ij}^{n} + \frac{\mathrm{Fo}'}{2(1+2\,\mathrm{Fo}')}\,[(U_{i+1j}^{n} + U_{i-1j}^{n} + U_{ij+1}^{n} + U_{ij-1}^{n}) + \delta\,(t_{i+1j}^{n} + t_{i-1j}^{n} + t_{ij+1}^{n} + t_{ij-1}^{n} - 4t_{ij}^{n})].$$

The components of the vectors t and U on the right-hand side of Eqs. (17) and (18) for the p + 1 iteration have already been determined and used for additional acceleration of the convergence of the iterative process.

In using Fourier analysis, the eigenvalues of the iterative matrices are determined; these are block-matrix eigenvalues

$$\mu^{t} = \frac{\mathrm{Fo}}{1+2\mathrm{Fo}}\cos\frac{\pi k}{J} + \frac{\mathrm{Fo}}{1+2\,\mathrm{Fo}}\cos\frac{\pi l}{I}, \tag{19}$$

$$\mu^{u} = \frac{\mathrm{Fo}'}{1+2\,\mathrm{Fo}'}\cos\frac{\pi k}{J} + \frac{\mathrm{Fo}'}{1+2\,\mathrm{Fo}'}\cos\frac{\pi l}{I}. \tag{20}$$

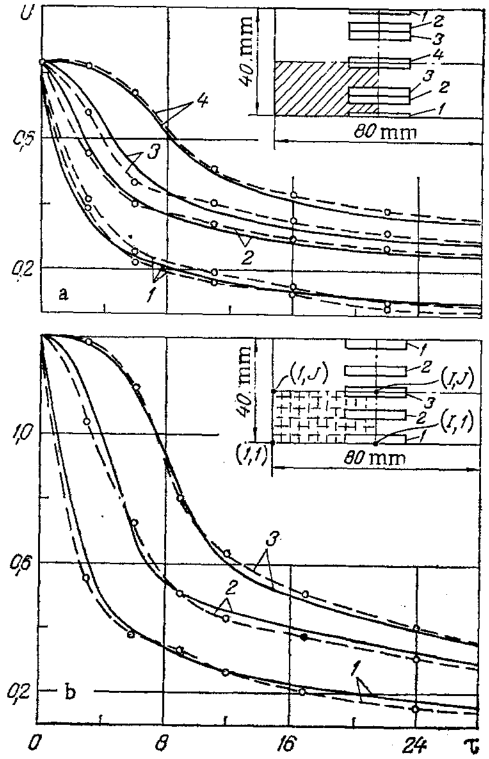

Fig. 2. Distribution of the moisture content U (kg/kg) with various experimental conditions (Fig. 1) in four (a, 1-4) and three (b, 1-3) elements of the experimental samples. The coefficients of the model: a) $D = 6.2\cdot 10^{-10}$; $v_{cap} = 7.8\cdot 10^{-5}$; $\lambda = 0.31$; $C = 2400$; $\rho_0 = 680$; $a = 1.6\cdot 10^{-7}$; $\varepsilon = 0.25$; $r_0 = 2.39\cdot 10^{6}$; $\alpha = 70$; $\alpha_u = 1.5\cdot 10^{-6}$; $\delta = 1.25\cdot 10^{-3}$; $\Delta = 4\cdot 10^{-3}$; $\Delta\tau = 1800$; b) $D = 8.7 \times 10^{-10}$; $v_{cap} = 7.5\cdot 10^{-5}$; $\lambda = 0.315$; $C = 2500$; $\rho_0 = 680$; $a = 1.66\cdot 10^{-7}$; $\varepsilon = 0.22$; $r_0 = 2.3\cdot 10^{6}$; $\alpha = 71$; $\alpha_u = 2.3\cdot 10^{-6}$; $\delta = 1.28\cdot 10^{-3}$; $\Delta = 4\cdot 10^{-3}$; $\Delta\tau = 1800$; continuous curves correspond to theory and dashed curves to experiment.

The maximum eigenvalues of the iterational matrices, which are used to optimize the relaxation parameter, are obtained when $\left|\cos\frac{\pi k}{J}\right|$ and $\left|\cos\frac{\pi l}{I}\right|$ are equal to unity, that is,

$$\mu_m^t = \frac{2\,\mathrm{Fo}}{1+2\,\mathrm{Fo}} < 1, \tag{21}$$

$$\mu_m^u = \frac{2\,\mathrm{Fo}'}{1+2\,\mathrm{Fo}'} < 1, \tag{22}$$

which proves the convergence of the iterational process.

The boundary conditions of the third kind are approximated in finite-difference form using the method proposed in [5] for convective heat transfer. Following this approach, the boundary conditions are written in the form: for the point (1, 1)

$$\frac{1}{2\,\mathrm{Fo}}\, t_{1,1}^{n+1} = t_{2,1}^n + t_{1,2}^n + \left(\frac{1}{2\,\mathrm{Fo}} - 2 - 2\,\mathrm{Bi}\right) t_{1,1}^n + 2\,\mathrm{Bi}\, t_a^n + 2\,\frac{(1-\varepsilon)\, r_0 \alpha_u \rho_0 \Delta}{\lambda}\,(U_e^n - U_{1,1}^n), \tag{23}$$

$$\frac{1}{2\,\mathrm{Fo}'}\, U_{1,1}^{n+1} = U_{2,1}^n + U_{1/2}^n + \left(\frac{1}{2\,\mathrm{Fo}'} - 2 - 2\mathrm{Bi}'\right) U_{1,1}^n + 2\,\mathrm{Bi}' U_e^n + \delta\,(t_{1,2}^n + t_{2,1}^n - 2t_{1,1}^n); \tag{24}$$

for the point (2, 1) and all the other surface points

$$\frac{1}{\mathrm{Fo}}\, t_{2,1}^{n+1} = t_{1,1}^n + t_{3,1}^n + 2t_{2,2}^n + \left(\frac{1}{\mathrm{Fo}} - 4 - 2\,\mathrm{Bi}\right) t_{2,1}^n + 2\,\mathrm{Bi}\, t_a^n + 2\,\frac{(1-\varepsilon)\, r_0 \alpha_u \rho_0 \Delta}{\lambda}\,(U_e^n - U_{2,1}^n), \tag{25}$$

$$\frac{1}{\mathrm{Fo}}\, U_{2,1}^{n+1} = U_{1,1}^n + U_{3,1}^n + 2U_{2,2}^n + \left(\frac{1}{\mathrm{Fo}'} - 4 - 2\,\mathrm{Bi}'\right) U_{2,1}^n + 2\,\mathrm{Bi}' U_e^n + \delta\,(t_{1,1}^n + t_{3,1}^n + 2t_{2,2}^n - 4t_{2,1}^n), \tag{26}$$

where $\mathrm{Bi} = \alpha\Delta/\lambda$; $\mathrm{Bi}' = \alpha_u\Delta/D$.

The following stability conditions are imposed on Eqs. (23)-(26): for the point (1, 1)

$$4(1+\mathrm{Bi})\mathrm{Fo}\leqslant 1,\ 4(1+\mathrm{Bi}')\mathrm{Fo}'\leqslant 1, \tag{27}$$

for the point (2, 1)

$$2(2+\mathrm{Bi})\mathrm{Fo}\leqslant 1,\ 2(2+\mathrm{Bi}')\mathrm{Fo}'\leqslant 1. \tag{28}$$

These constraints considerably reduce the efficiency of numerical solution. If the components of the vectors t and U at the boundary of the body are calculated in the iterative procedure for any iteration, with a step $\Delta\tau$ satisfying the stability condition, and the matrix Eqs. (13) and (14) are solved with a large time step, the efficiency of solution is high, but there is a known loss in accuracy.

Numerical experiment shows that the loss in accuracy is within limits of 2-3°C for t and 0.02 kg/kg for U. This corresponds to the accuracy with which t and U may be measured in practice. The accuracy of solution improves with small changes in the parameters of the surrounding medium.

Order of Calculation

1. When the components of U at the grid points on the surface are less than U_f, but larger than U_f inside the body, the vector U is determined explicitly by Eqs. (8)-(12), and t by Eq. (17).

2. When the components of U are less than U_f at points on the surface and partially at internal grid points, the computational procedure is performed with several steps. From the components of t and U determined at the preceding time step, the vectors V_{ij} and W_{ij} are formed; W_{ij} is formed as long as $U_{ij} \leqslant U_f$. In the next time step, P iterations are performed with respect to Eqs. (17) and (18), together with the boundary conditions in Eqs. (23)-(26). The iterative process for Eqs. (17) and (18) is performed until $U_{ij} \leqslant U_f$. After the completion of the iterative process, the components of the vector $U > U_f$ for the remaining points are determined from Eqs. (8)-(12). In the region of the hygroscopic state, the vectors t and U are determined from the boundary conditions and the iterative schemes in Eqs. (17) and (18) for all the grid points.

Discussion of the Results

The temperature and moisture content in beechwood were measured experimentally, with the following parameters of the surrounding medium: t_α = 50°C and φ = 0.73, 0.48, 0.37; t_α = 60°C and φ = 0.75, 0.57, 0.42; t_α = 80°C and φ = 0.81, 0.63, 0.42.

Appropriate sealing of the ends of the experimental samples provides conditions for two-dimensional water transport in a direction perpendicular to the beechwood grain. The temperatures t_α, T_M, and t_c are measured by Pt 100 platinum thermoresistors and their values are recorded on the tape diagram of a six-point measuring bridge of accuracy class 0.5. In the course of the process, the mean moisture content of the elements corresponding to the precisely determined number of grid points is measured by a weight method.

The elements are cut from a section obtained from the experimental sample after a definite amount of drying time.

The variation in $\bar{U}$ and t_c in two experiments with beechwood samples is shown in Fig. 1. Two periods of the drying process are observed: one at a constant rate and one at a decreasing rate. In the first period, t_c is approximately equal to t_M; in the second, T_c tends asymptotically to t_α. The mean square deviation between the theoretical and experimental values of $\bar{U}$ is in the range from ±0.017 to ±0.022 kg/kg.

The time dependence of the moisture content in the same two experiments is shown in Fig. 2. The mean square deviation for $\bar{U}$ in this case is within ±0.045 kg/kg.

Solving the inverse problem, a correlational dependence of v_{cap} on φ may be obtained in the form

$$v_{cap} = 10^{-(2.5517\varphi+4.9586)}. \tag{29}$$

The results obtained permit the conclusion that Eq. (5), together with Eqs. (1) and (2), is a mathematical model of the heat and moisture transfer in capillary-porous colloidal bodies for the description of the hygroscopic and wet states.

LITERATURE CITED

1. A. V. Lykov, Heat and Mass Transfer (Handbook) [in Russian], Énergiya, Moscow (1978).
2. A. V. Lykov and Yu. A. Mikhailov, Theory of Heat and Mass Transfer [in Russian], Gosénergoizdat, Moscow (1963).
3. D. E. Potter, Computational Physics, Wiley (1973).
4. G. S. Shubin, Physical Principles and Calculation of Wood Drying Processes [in Russian], Lesnaya Promyshlennost', Moscow (1973), pp. 23-180.
5. W. M. Rohsenow and J. P. Hartnet, Handbook of Heat Transfer, McGraw-Hill, New York (1973), pp. 4/50-4/78.
6. H. R. Thomas, R. W. Lewis, and K. Morgan, "An application of finite-element method in the drying of timber," Wood Fib., 11, No. 4, 237-243 (1980).
7. T. F. Siau, Flow in Wood, Syracuse Univ. Press, New York (1971).

NUMERICAL SIMULATION OF PROCESSES IN A SPHERICAL COMBUSTION CHAMBER

A. I. Marchenko and G. S. Romanov

UDC 533+539

A theoretical model of gasdynamic and mechanical processes in a spherical explosion chamber is considered. Comparison of numerical results obtained with this model with calculated and experimental results of other authors shows good agreement.

The present study will describe a method for numerical simulation of the processes which take place in a spherical explosion chamber by using the equations of the mechanics of continuous media without consideration of the differing natures of dissipative effects (radiant diffusion, turbulence, etc.) which can play a significant role in real conditions. The model to be considered permits description of both gasdynamic processes within a chamber caused by expulsion and braking of material from the energy source, and elastic compression waves — expansion of the medium under dynamic loading of the chamber walls at stresses not exceeding the strength of the wall material, i.e., for situations of practical interest [1, 2].

The proposed model was used to study processes in an explosion chamber which consisted of three spherically symmetric regions: 1) a central region 3 cm in diameter (energy source) with density $\rho_1 = 2.7$ g/cm^3 and mass $3.054 \cdot 10^2$ g, within which an energy of $E_0 = 7.106 \cdot 10^9$ J is liberated instantaneously corresponding to a specific internal energy of $E = 2.327 \cdot 10^7$ J/g; 2) an air layer of thickness ~ 2 m with gas density $\rho_0 = 1.293 \cdot 10^{-3}$ g/cm^3 and pressure $P_0 = 1$ atm; 3) a medium surrounding the air cavity (aluminum with density of $\rho_1 = 2.7$ g/cm^3 was chosen for the chamber wall material).

Since the problem under study allows similarity transformation of the linear R_* and time t_* scales with the relationships $R_* \sim E_0^{1/3}$ and $t_* \sim E_0^{1/3}$, some of the results obtained were compared with data of [2] for an explosion of energy $E_0 = 7.106 \cdot 10^{12}$ J in an air cavity of radius $R_0 = 20$ m.

The thermodynamic parameters of the air layer were calculated with a tabular equation of state $P = P(E, \rho)$, obtained by linear interpolation in logarithmic variables using the data of [3]. The media in the first and third regions were described by Tillotson's equations [4-6], which are recommended for calculation of high-velocity shocks on metal and plastic targets [5], which corresponds to real conditions on the chamber walls. The well-known equations of [7, 8], which relate deformation and stresses produced by action of shock wave pulses on the chamber walls, were used to consider the mechanical properties of the surrounding medium (chamber walls).

In describing wave motion in the chamber and walls, strength and other inelastic phenomena, nonequilibrium properties, and radiation characteristics of the medium will be neglected, which, according to [2], is completely justifiable.

A. N. Sevchenko Scientific-Research Institute of Applied Physics Problems, V. I. Lenin Belorussian State University, Minsk. Translated from Inzhernerno-Fizicheskii Zhurnal, Vol. 47, No. 4, pp. 657-662, October, 1984. Original article submitted April 27, 1983.

 0022-0841/84/4704-1230$08.50